RSC Advances

ROYAL SOCIETY OF CHEMISTRY

www.rsc.org/advances

Journal Name

RSCPublishing

ARTICLE

Cite this: DOI: 10.1039/x0xx00000x

Organic fluorine involved intramolecular Hydrogen Bonds in the derivatives of Imides: NMR Evidence corroborated by DFT based theoretical calculations

Received 00th January 2012,
Accepted 00th January 2012

DOI: 10.1039/x0xx00000x

www.rsc.org/

Sandeep Kumar Mishra and N. Suryaprakash*

The rare occurrence of the intramolecular Hydrogen bonds (HBs) of the type N−H•••F−C are detected in the derivatives of imides in a low polarity solvent by using multi-dimensional and multinuclear NMR experiments. The observation of $^{1h}J_{FH}$, $^{2h}J_{FN}$, and $^{2h}J_{FF}$, where the spin magnetization is transmitted through-space among the interacting NMR active nuclei, provided the strong and unambiguous evidence for the existence of intra-molecular HB. The variation of chemical shifts of labile protons on physical conditions, such as, solvent dilution and systematic alteration of temperature confirmed the presence of weak interactions through intramolecular HBs in all the investigated fluorine substituted molecules. The self or cross dimerization of molecules is unequivocally discarded by the analysis of the rates of diffusion obtained using pseudo-two dimensional DOSY experiments. The Density Function Theoretical (DFT) calculations based on Quantum Theory of Atoms in Molecules (QTAIM) and Non Covalent Interaction (NCI), are in close agreement with the NMR experimental findings.

Introduction

Among several inter- and intra- molecular interactions which are inherently present in diverse molecules, the weak hydrogen bonds (HBs) occupy special place in chemistry and biology.[1-4] The importance of HB in the self-assembly of molecules[5-17] is well documented in the literature. The majority of the reported intramolecular HB mainly pertains to motifs of the type O···H-N and N···H-N[18-22]. Furthermore it is well known that nearly 30% of the commercially available drug molecules contain at least one fluorine atom. In addition, the organofluorine molecules have enormous importance due to their applicability as biomaterials, agro chemicals, in molecular imaging,[23, 24] crystal engineering[25-27] and also in the functional materials designing[28]. The bio-origin of medicinal and bio-inorganic property of fluorinated compounds is a consequence of the binding nature of fluorine to enzyme active sites[29-33] through intermolecular hydrogen bonded bridges of the type X-H···F-C (X=O, N). Nevertheless there are very few reports of the participation of organic fluorine in the HB in solution state[34-36]. The nuclear magnetic resonance (NMR) and X-ray crystallographic studies have been reported on the N-H···F-C HB in foldamers and benzanilides[37,38]. It is also well known that organic fluorine generally does not get involved in the intramolecular HB[39-45]. The report by

Dunitz and co-workers concluded that ''organic fluorine hardly ever accepts hydrogen bonds''[46-49]. As far as the HB in the solution state is concerned, the first NMR spectroscopic report involving organic fluorine was reported by detecting the through space coupling ($^{1h}J_{FH}$)[50] mediated by HB. Subsequently Limbach and his co-workers have made enormous contributions for the development of this field and have explored several examples where not only organic fluorine but also other halogens participated in the intermolecular HB[51-54]. Exclusive NMR studies on the existence of intramolecular HB of the type, X-H···F-C (X=O, N), in the solution state, have been reported in benzanilide and benzamide[44,45] derivatives. Our group has recently utilized NMR technique and detected the participation of organic fluorine in the intramolecular HB in the derivatives of hydrazides and bisoxamides[55,56]. In continuation of the ongoing research in our group, in the present work we are reporting the extensive studies carried out on the fluorine substituted derivatives of imides. The imides are the diacyl derivatives of ammonia or the primary amines[57]. Different derivatives of imides have been proven to be very important in, high strength electrically conductive polymers[58-60], synthetic applications[61], medicinal activity[62], as ionic fluids[63], in pharmacology[64] and as synthetic precursors[65]. The NH linker of an imide provides ample scope to synthesize different derivatives with the desired substitution on acyl group(s). The procedure for their synthesis is already available in the literature[62,66,67]. In the present study we have synthesised the selected derivatives of imides using microwave assistedmethod[66] of imide synthesis and characterized them by extensive utility of NMR techniques and ESI-HRMS spectrometry. The chemical structures of the investigated molecules are reported in the scheme 1. These molecules can be classified into two categories, symmetric ones where X=X' (molecules **1-3**) and the asymmetric ones where X≠X' (molecules **4-7**). The NMR derived information on intramolecular HB has been unequivocally supported by Density Function Theory (DFT)[68, 69] based Non Covalent Interaction (NCI)[70], and Quantum Theory of Atom in Molecule (QTAIM)[71] calculations.

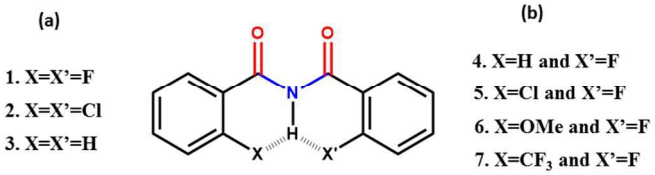

Scheme 1. The chemical structures of the derivatives of 2-X-*N*-(2-X'-benzoyl)benzamide.

Results and discussion

The basic information on HB can be derived by monitoring the variation in the chemical shift in the NMR spectrum as a function of the physical parameters, such as, systematic variation in the temperature or solvent dilution. The hydrogen bonded proton will have its resonance peak shifted towards downfield consequent to the decrease in the electron density surrounding it. This change in chemical shift arises due to the variation in the concentration, alteration in the polarity of the solvent, and the temperature alteration. In order to distinguish the intra- and inter- molecular HB and to monitor the effect of atmospheric monomeric water on HB, the solvent titration experiments[34-36, 72] were performed on the molecules **1-7** in the solvent $CDCl_3$. The plot of variation of the chemical shift as a function of solvent concentration is reported in Fig. 1A. From this figure it is clearly evident that there is not any significant change in the chemical shift of NH proton in the ^{1}H NMR spectra, thereby discarding the possibility of intermolecular HB, aggregation or dimerization. In addition the chemical shift of ^{1}H resonance of water was invariant confirming the negligible effect of monomeric water on the intramolecular HB[73].

High polarity solvent dimethyl sulphoxide (DMSO) is a very good HB acceptor and hence it can rupture the variety of inter- and intra-

molecular HBs[44,45]. To derive the qualitative information on the relative strengths of intramolecular HB the titration study with the solvent DMSO-d_6 was carried out on the molecules **1-7**. The variation of the chemical shift of NH proton as a function of solvent concentration is reported in Fig. 1B. The excessive deshielding of NH proton is observed due to the disruption of intramolecular HB[44,45] due to the strong interaction with DMSO. Interestingly the molecule **6** exhibited the upfield shift for NH peak on addition of DMSO indicating that, in this particular example, the intramolecular HB formed between oxygen atom of the methoxy group and NH proton might to be stronger than its interaction with DMSO[55].

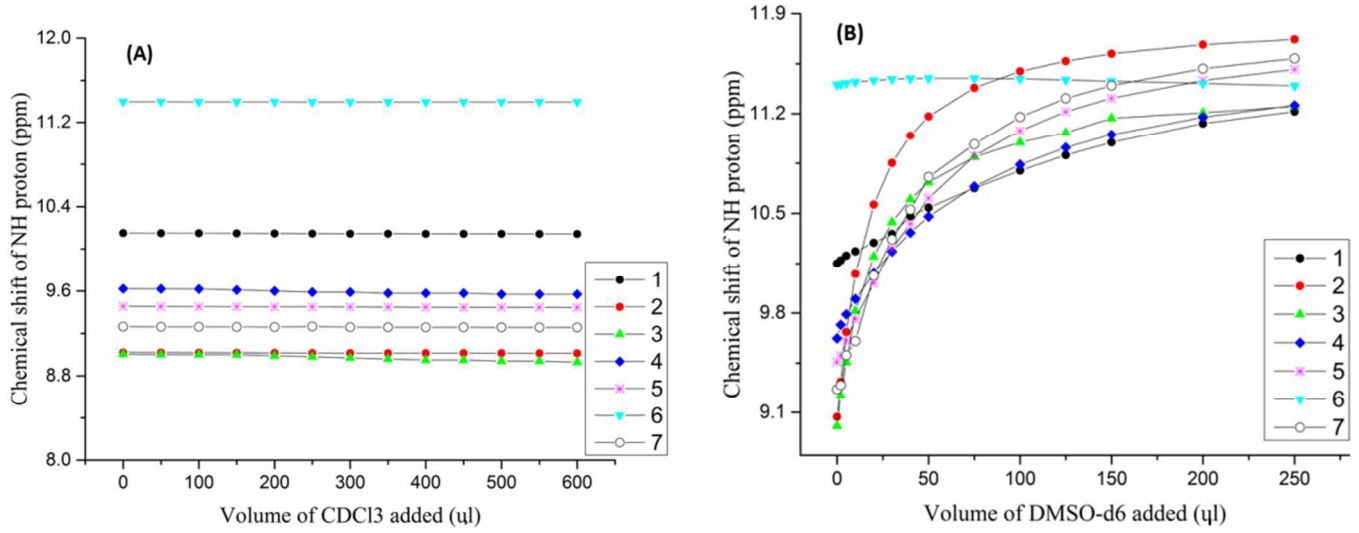

Figure 1. (A,B) The variation in chemical shifts of NH protons as a function of volume of $CDCl_3$ and the volume of DMSO-d_6 respectively for the molecules **1-7.** The initial concentration taken was 10 mM in the solvent $CDCl_3$. **(A)** The plot of NH chemical shift with the incremental addition of $CDCl_3$ to an initial volume of 450 µl, at 298 K. **(B)** The incremental addition of DMSO-d_6 to an initial volume of 450 µl in $CDCl_3$, at 298 K**.** The molecules **1-7** are identified by the symbols given in the inset.

The strength of HB gets increased on lowering the temperature. As a result the deshielding of the NH proton in the ^{1}H NMR spectrum is observed due to the larger displacement of hydrogen bonded proton towards the HB acceptor, providing an evidence of intramolecular HB[74-76]. The chemical shift of NH protons as a function of temperature (over the range of 298-220 K) for molecules **1-7** are compiled in Fig. 2A. The downfield shift of the NH proton resonance on lowering the temperature is observed due to strengthening of HB.

Another interesting feature observed is the change in FH coupling value in the ^{1}H NMR spectrum. Such a variation is detected only when the organic fluorine is interacting with the NH proton mediated through HB. The variation in the coupling constant (through space) as a function of temperature is reported in the Fig. 2(B), for the molecules **1** and **4-7.** This phenomenon provides the strong evidence in favour of HB.

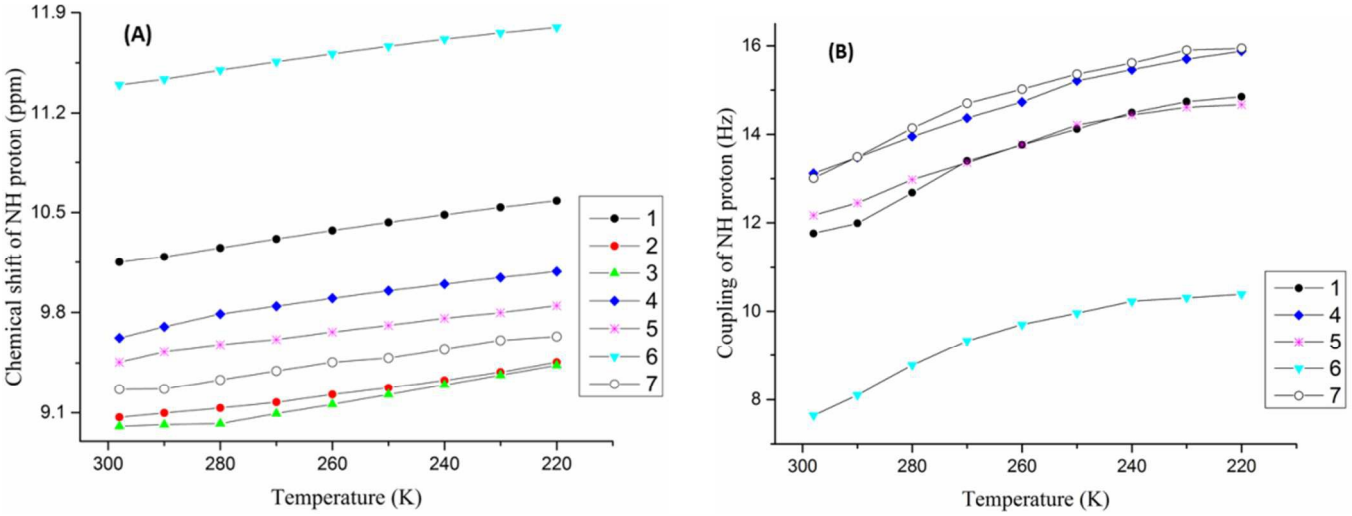

Figure 2. Variation of (A) chemical shifts of NH protons as a function of temperature for the molecules **1-7** and (B) the through space mediated HF coupling constant as a function of temperature for the molecules **1** and **4-7.** The molecules are identified by the symbols given in the inset**.** The initial concentration was 10 mM in the solvent $CDCl_3$.

The variation in the chemical shift values during titration studies are assimilated in Table 1. The ^{1}H NMR chemical shifts derived using GIAO[77] and CSGT[77], DFT methods of NMR simulation were compared with experimentally determined ^{1}H NMR chemical shifts of NH protons for the molecules **1-7**. It is observed that the CSGT method is giving the values that are in close agreement with the experimental values. The calculated values using CSGT method are compiled in Table 1.

Table. 1. The solvent and temperature dependent changes in the chemical shifts, through space couplings for the molecules **1-7.** The chemical shift (ppm) of NH protons is theoretically calculated using CSGT method of NMR simulation in default-chloroform solvation medium. The reported experimentally determined chemical shifts (ppm) for the molecules **1-7** are in the solvent $CDCl_3$.

Molecule	HB type (X····HN)	Change in chemical shift (ppm)			Change in through-space coupling (Hz)	Theoretical Chemical shift of NH proton (ppm)	Experimental Chemical shift of NH proton (ppm)
		On adding 600 µl $CDCl_3$	On adding 250 µl DMSO	Temperature varied from 298 to 220 K	Temperature varied from 298 to 220 K		
1	(F···HN)	-0.0052	1.0423	0.4309	3.09	9.8	10.15
2	(Cl···HN)	-0.0079	2.6999	0.2868		9.0	9.07
3	(H···HN)	-0.0739	2.2485	0.3456		9.2	9.00
4	(F···HN and H···HN)	-0.0063	1.5813	0.46225	1.98	9.5	9.62
5	(F···HN and Cl···HN)	+0.00135	2.0087	0.3917	2.44	9.4	9.46

6	(F···HN and MeO···HN)	-0.0008	-0.0954	0.4001	2.75	10.5	11.40
7	(F···HN and CF_3··HN)	-0.0062	2.2942	0.3076	2.67	9.2	9.26

There is a possibility that molecules of this type might undergo self-dimerization. The absence of any type of dimerization of the investigated molecules was confirmed by pseudo two dimensional ^{1}H DOSY[78,79] experiments and ESI-HRMS analysis. Since it is well known that the molecule 2-methoxy-N'-(2-methoxybenzoyl)benzohydrazide labelled as **8** in Fig. 3**,** does not show any type of self-dimerization or aggregation[55], even in 20 mM solution. The ^{1}H-DOSY NMR experiment was therefore carried out for a mixture of 1:1 molar ratio (20 mM final solution) of molecules **8** and **1** in the solvent $CDCl_3$. The corresponding DOSY spectrum is reported in Fig. 3.

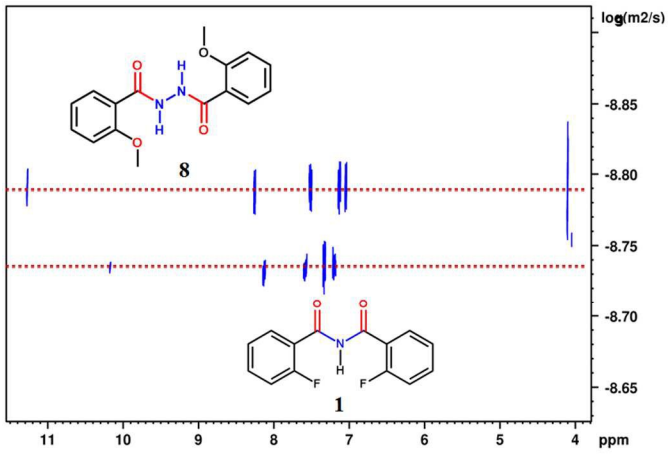

Figure 3. 500 MHz ^{1}H-DOSY NMR spectrum of 20 mM solution of the mixture of molecules **8** and **1** at a 1:1 molar ratio in the solvent $CDCl_3$.

From the Fig. 3 one can visualize that both the molecules have different coefficients of diffusion. Furthermore the rate of diffusion for the molecule **8** is slower than the molecule **1**, as expected in the absence of any aggregation or self-dimerization by molecule **1**. Thus it conclusively eliminates any possibility of self- or cross-dimerization.

The unambiguous evidence for the existence of HB can be obtained by detecting through space couplings between hydrogen bonded NMR active nuclei, where the magnetization transfer takes place through hydrogen bond. The one and two dimensional homo- and hetero- nuclear NMR correlation experiments can be employed for the detection of through space couplings, where the spin polarization is transferred across the hydrogen bond[80-83]. The 1/2 spin and 100% natural abundance of ^{19}F renders it a favourable nucleus for NMR detection. Thus the various NMR experiments involving ^{19}F were carried out. The ^{1}H and ^{1}H{^{19}F}[45] spectra of molecule **1** in the solvent $CDCl_3$, and the ^{1}H spectrum in the solvent DMSO-d_6 are given in Fig. 4. The NH peak of the molecule **1** is a triplet with the separation between the adjacent transitions of the triplet corresponding to 13.03 Hz (Fig. 4a). This triplet collapses into a singlet in ^{1}H{^{19}F}[45] experiment confirming the presence of coupling between ^{1}H and ^{19}F (Fig. 4b). Such a large value of the coupling mediated through covalent bond ($^5J_{FH}$) between ^{1}H and ^{19}F is very unlikely[44,45] and the most likely possibility would be mediated through HB ($^{1h}J_{FH}$). This is further ascertained by acquiring the spectrum in a high polarity solvent DMSO-d_6 which resulted in the collapsing of triplet to a singlet (Fig.4c).

Journal Name RSCPublishing

ARTICLE

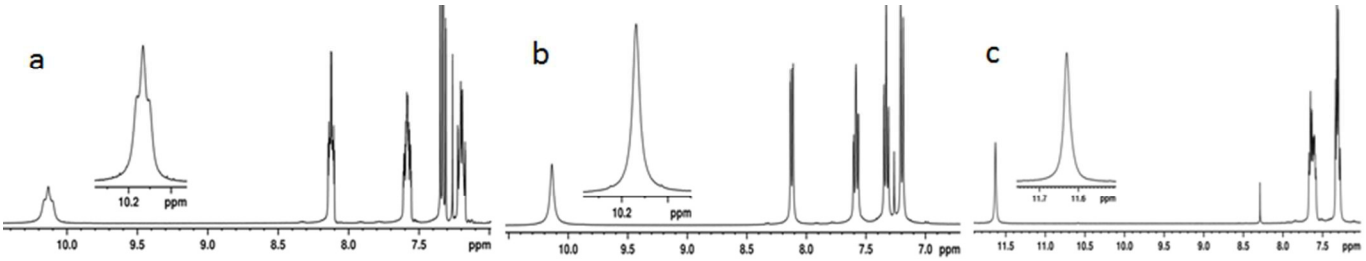

Figure 4: 400 MHz ^{1}H NMR spectra of molecule **1**; **a)** in the solvent $CDCl_3$; **b)** $^{1}H\{^{19}F\}$ in the solvent $CDCl_3$; and **c)** ^{1}H NMR spectrum in the solvent DMSO-d_6.

For obtaining stronger evidence for the involvement of organic fluorine in the intramolecular HB we have carried out the 2D NH-coupled and ^{1}H decoupled ^{1}H-^{15}N HSQC NMR experiment, where ^{15}N is present in its natural abundance. The corresponding spectra for molecule **1** are reported in Figs. 5(a) and 5(b) respectively. The coupled ^{1}H-^{15}N-HSQC spectra are also helpful in assigning the relative signs of couplings mediated through HB. The measured through space couplings in both direct and indirect dimensions of HSQC spectrum are labelled with alphabets and their values with the relative signs are also reported in the spectrum. The observation of through space couplings of significant larger strengths, such as, $^{1h}J_{FH}$ and $^{2h}J_{FN}$ gives strong and direct evidence on the involvement of organic fluorine in the intramolecular HB. The NH-coupled ^{1}H-^{15}N HSQC experiment was also carried out in the solvent DMSO-d_6 and the corresponding spectrum is reported in Fig. 5(c). In the solvent DMSO, except for $^{1}J_{NH}$, all the other couplings disappeared. This gives another strong and unambiguous evidence that the measured couplings $^{1h}J_{FH}$ and $^{2h}J_{FN}$ in the solvent $CDCl_3$ are mediated through HB. The ^{1}H-^{15}N HSQC spectra of all the other investigated molecules, along with the measured magnitudes and relative signs of the couplings are reported in ESI.

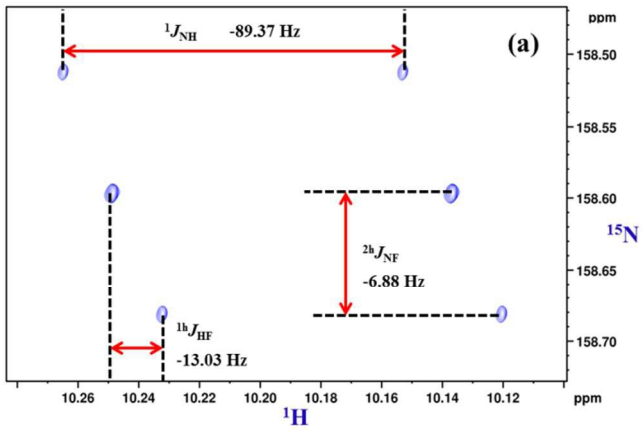

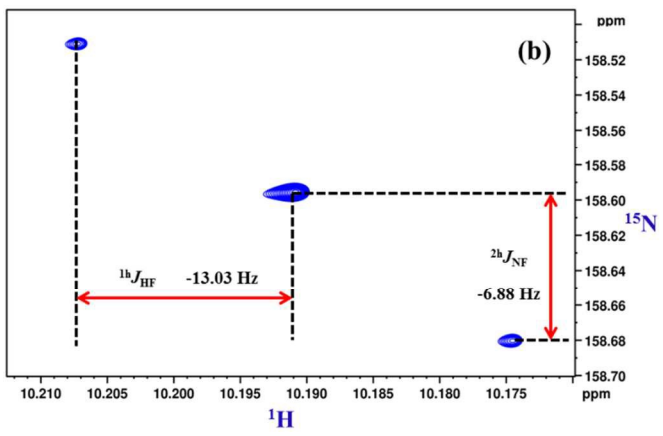

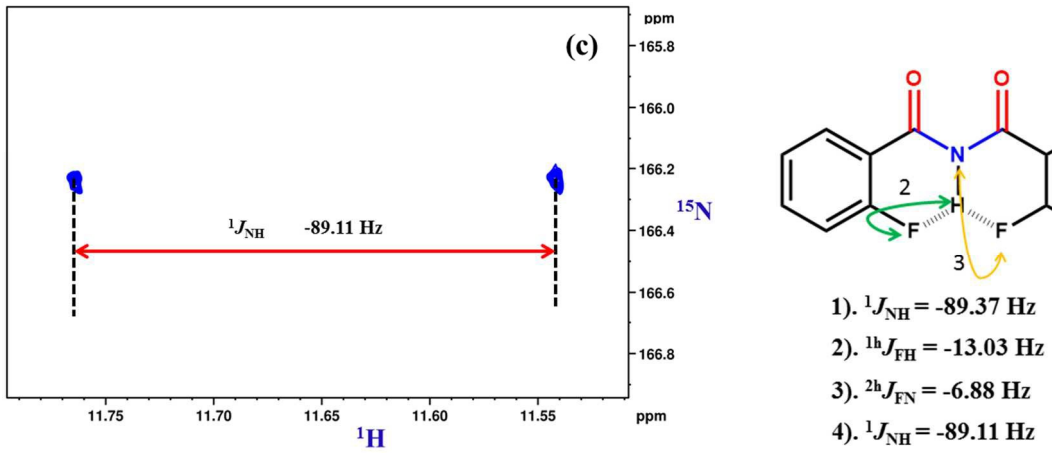

Figure 5. 800 MHz spectrum of molecule **1** in the solvent $CDCl_3$ (a) ^{1}H-^{15}N-HSQC (NH-coupled); (b) ^{1}H-^{15}N-HSQC (NH-decoupled); **(C)** 400 MHz ^{1}H-^{15}N-HSQC spectrum (NH-coupled) in the solvent DMSO-d_6. The chemical structures with the magnitudes of scalar and through space couplings are identified by double headed arrows. The measured coupling values and their relative signs derived from the relative slopes of displacement of cross sections are also given.

From Figs. 5(a) and 5(b) the magnitudes and the relative signs of the couplings could be derived. Based on the earlier reports[44, 45] the relative signs of $^{1h}J_{FH}$ and $^{2h}J_{FN}$ are assigned to be negative. All the measured magnitudes of the couplings along with their appropriate signs are reported in Fig. 5.

There is also a great significance in the value of $^{1}J_{NH}$ in understanding the nature of HB. The extent of $^{1}J_{NH}$ will increase if HB is predominantly electrostatic[84] and decrease if the HB is predominantly a covalent type[85]. The $^{1}J_{NH}$ values of all the investigated molecules obtained from NH coupled ^{15}N-^{1}H HSQC experiments in the solvent $CDCl_3$ are compiled in Table 2. The visual comparison of $^{1}J_{NH}$ couplings of all other molecules with that of an unsubstituted molecule **3**, it is evident that the $^{1}J_{NH}$ couplings of the substituted molecules **1, 2** and **4-7** are substantially smaller than the molecule **3**, providing strong and unambiguous evidence that the nature of HBs in the derivatives of imides is predominantly of the covalent type.

The nuclear Overhauser (nOe) effect can also be used to correlate the strength of intramolecular HB in the molecule. The spatial proximity between two spins involved in dipolar interaction is correlated with the change in intensity of peak in two dimensional nuclear Overhauser effect spectrum. Thus the 2D ^{1}H-^{19}F hetero nOe spectroscopy (HOESY)[86-88] experiments were carried out for all the fluorine containing molecules **1** and **4-7**, where the through space correlation is established between NH proton and the F atom. The hexafluorobenzene (C_6F_6) is used as an internal reference for all the ^{19}F spectra. The 2D ^{1}H-^{19}F HOESY spectrum of the molecule **1** is reported in the Fig. 6b. The HOESY spectra of other molecules, **4-7** are reported in ESI. The close spatial proximity between F and NH proton is established by detecting the correlated peak between NH proton and F atom in all the molecules. Thus the results derived from the different NMR experiments provided strong evidence for the involvement of organic fluorine in the intramolecular HB in all the investigated fluorine containing molecules.

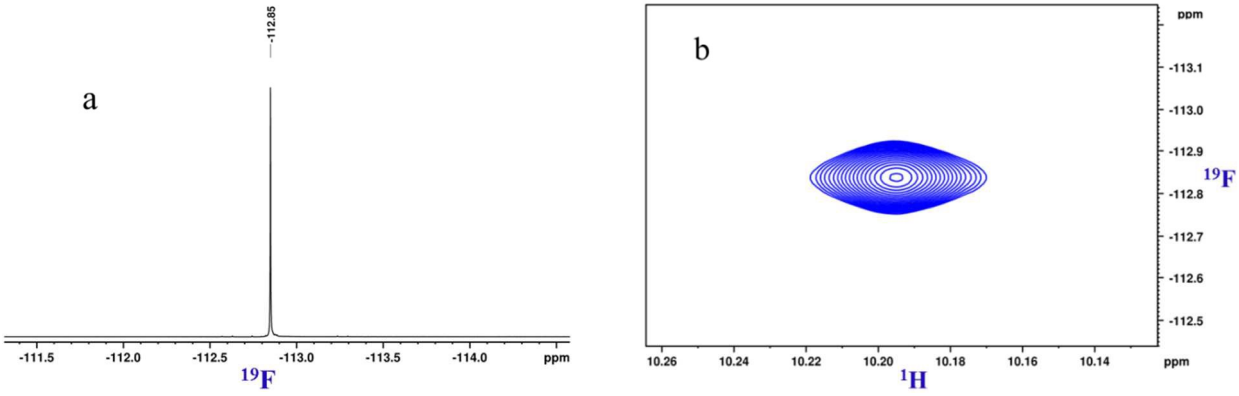

Figure 6. 376.5 MHz (a) ^{19}F and (b) 2D ^{1}H-^{19}F HOESY spectra of the molecule **1** in the solvent $CDCl_3$.

Theoretical calculations

The molecular weak interactions established by NMR experimental findings were also further corroborated by DFT[68, 69] optimized structure based theoretical calculations. To optimize the lowest energy structures for the investigated molecules **1-7** the DFT calculations were performed using Gaussian09 suit,[89] with B3LYP/6-311+g (d,p) level of theory with the default-chloroform as the solvation medium. The harmonic vibrational frequency values were utilized to obtain the minimum energy structures. The coordinates of these energy minimised molecular geometries were used to generate the wave function files for QTAIM, and NCI studies.

Non Covalent Interaction (NCI) Calculations

The powerful non covalent interaction (NCI)[90] approach is used to detect non covalent interactions in real space which is dependent on the electron density and its derivatives. It provides a strong representation of the steric repulsion, van der Waals interactions and the HBs. There is a very large positive gradient of the reduced density gradient (RDG), and the RDG values will be small, approaches zero in the density tail (i.e., regions far from the molecule, where the electron density exponentially decays to zero). This is the condition for both the covalent and non-covalent bonding regions. There is a strong correlation of electron density ($\rho_{(r)}$) with the weak interactions in the corresponding regions. The correlations for the HB are negative and positive for the steric effect, while the van der Waals interaction will always have very small $\rho_{(r)}$ values[90] (near to zero). The calculated grid points are plotted for a defined real space function, $sign(\lambda_{2(r)})\rho_{(r)}$, as function 1 and reduced density gradient (RDG) as function 2 using Multiwfn[91] program for the molecules **1-7**. The program VMD[92] is used for plotting colour filled isosurfaces from these grid points. The plot for the $sign(\lambda_{2(r)})\rho_{(r)}$ v/s RDG, and the coloured isosurfaces for the molecule **1** are reported in Figs. 7a and 7b respectively.

Journal Name RSCPublishing

ARTICLE

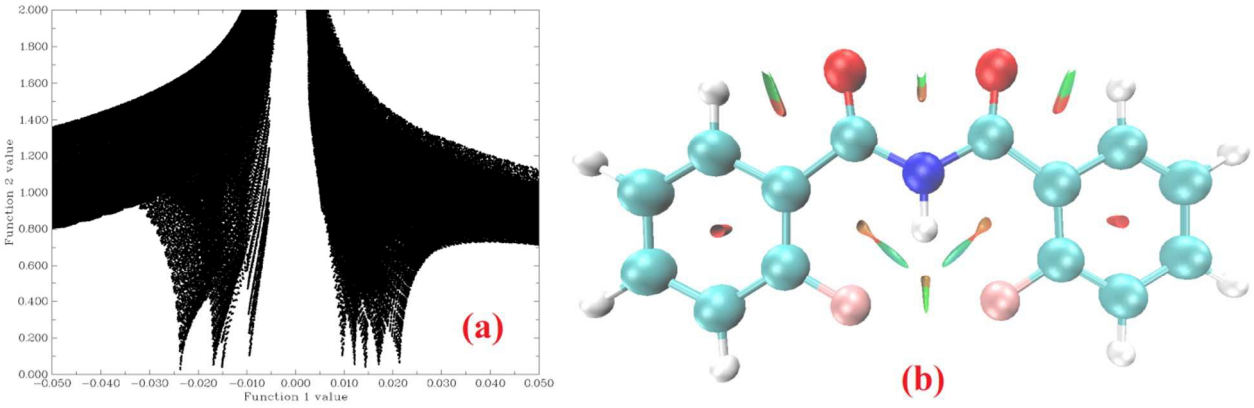

Figure 7. (a) The plot of sign(λ_2(r))*ρ(r) as function 1 v/s the RDG as function 2, and (b) coloured isosurface plot (green colour denotes weak H-bond and red colour stands for steric effect) for molecule **1**. The plots for remaining molecules, **2-7** are given in the supporting information.

The four spikes on the left hand side in Fig.7a (i.e. sign(λ_2(r))*ρ(r) negative) for the molecule **1** denotes four types of weak interactions, viz., N-H···F, C-H···O, F···F and a very weak O···O. These four HBs can be visualized in Fig. 7b as isosurfaces of green colour. The red coloured isosurface in plot (Fig.7b) represents the steric interactions arising from aromatic phenyl ring and other HB mediated rings. This is seen as five spikes in the Fig.7a on the right hand side (i.e. sign(λ_2(r))*ρ(r) is positive) . The similar plots and discussions for the remaining molecules **2-7** are reported in the supporting information.

Atoms in molecules (AIM) calculations

After confirming the presence of HB by NCI plot, the energy of interaction must be known for in depth understanding of the molecular properties influenced by weak HBs. The topology analysis technique was reported as "atoms in molecules" (AIM) theory, and also cited as "the quantum theory of atoms in molecules" (QTAIM)[71, 93-96] dependent on the quantum observables (electron density $\rho_{(r)}$ and the energy densities). The points (except at infinity) where gradient norm of function value is zero are called as critical points (CPs) in topology analysis. According to the negative Eigenvalues of Hessian matrix of real space function[71, 93-96] CPs can be of four types. Out of them the (3,-1) CP is called as bond critical point (BCP). There is a great significance of the value of real space function at BCP. For example the bond strength and bond type respectively are related closely to the value of electron density ($\rho_{(r)}$) and the sign of Laplacian of electron density ($\nabla^2\rho_{(r)}$) at BCPs[71, 93-96]. The magnitudes of $\rho_{(r)}$ and signs of $\nabla^2\rho_{(r)}$ for BCP of HBs of interest are calculated using AIM calculations and

compiled in Table 2. At corresponding (3, -1) critical points (r_{cp}) the gradients of electron density ($\rho_{(r)}$) get vanished. The energy of HB (E_{HB}) is directly related to potential energy density ($V_{(r)}$) by straightforward relationship[97] $E_{HB}=V(\mathbf{r}_{bcp})/2$. The E_{HB} of X•••HX type HB can be calculated by using this relationship. The calculated values of E_{HB} for all the located BCPs of interest are assimilated in Table 2.

Conformational study

The molecules of investigated imides can exhibit conformational isomerism and the number of such possible isomers is dependent on the substitution on the phenyl ring. For the investigated molecules maximum of 3-4 conformers are possible, which are shown in the scheme below.

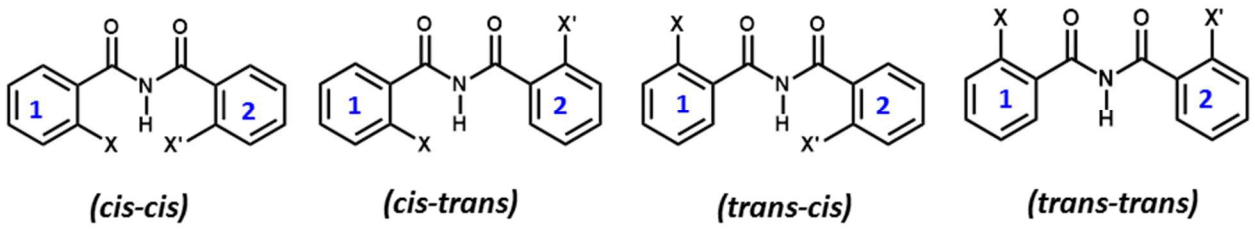

Scheme 2: The possible conformers of the investigated imide molecules arising due to ring flip.

Out of the four possible conformers the conformers cis-cis and trans-trans were optimized using Gaussian09 suit,[89] with B3LYP/6-311+g (d,p) level of theory with the default-chloroform as the solvation medium and the difference ((cis-cis) – (trans-trans)) of minimum energy was taken. The energy difference $\Delta E_{cis\text{-}trans}$ of all the investigated molecules is listed in Table 2. From the Table 2 it is evident that the energy of cis-cis conformers is always lower than the trans-trans that are due to the presence of HB.

Table 2. Electron density ($\rho_{(r)}$) and Laplacian of electron density ($\nabla^2\rho_{(r)}$) at different BCPs of type (3, -1) for (X····HN) H-bond and the energy of particular H-bonds calculated on the basis of potential energy density ($V_{(r)}$) are listed. The calculations were done using solvation medium of default-chloroform. The $^1J_{NH}$ was measured in the solvent $CDCl_3$.

Molecule	HB type (X··HN)	Electron density ($\rho_{(r)}$) (a.u.)	Laplacian of electron density ($\nabla^2*\rho_{(r)}$)	Energy of HB (E_{HB}) (Kcal/mol)	Energy difference (cis-trans) $\Delta E_{cis\text{-}trans}$ (Kcal/mol)	$^1J_{NH}$ in the solvent $CDCl_3$
1	(F··HN)	0.0237	0.1006	-6.4283	-10.97	-89.37
2	(Cl··HN)	0.0179	0.0617	-3.4298	-1.88	-88.07
	(Cl---Cl)	0.0109	0.0444	-2.0711		
3	(H··HN)	0.0297	-0.8246	a		-86.43

4	(F··HN)	0.0268	0.1127	-7.4767	-6.33	-88.22
	(H··HN)	0.0145	0.0568	-2.7708		
5	(F··HN)	0.0209	0.0870	-5.5176	-7.63	-89.17
	(Cl··HN)	0.0217	0.0723	-4.4714		
	(F---Cl)	0.011	0.0483	-2.6671		
6	(F··HN)	0.0184	0.0777	-4.7723	-10.68	-89.59
	(MeO··HN)	0.0326	0.1300	-8.9233		
7	(F··HN)	0.0256	0.1083	-7.0360	-3.83	-88.52
	(CF_3··HN)	0.0107	0.0424	-2.5233		

[a] shared-shell interaction because the Laplacian of electron density is negative.

The visualization of BCPs and bond paths of HBs for the molecule **1** is reported in the Fig. 8 and for the other investigated molecules **2-7** in ESI.

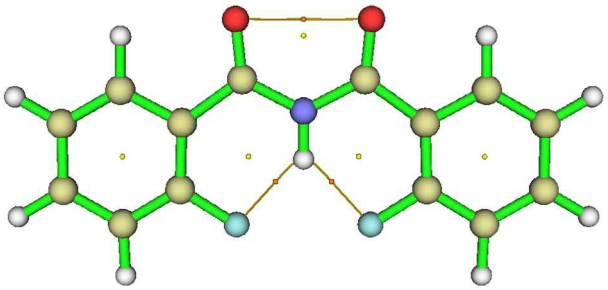

Figure 8: The visualization of BCPs and bond paths of HB for the molecule **1** plotted using multiwfn software. Dots represent the CPs and thin bar represents the HB interactions.

The presence of significant interactions at (3,-1) BCPs are confirmed by significantly large values of $\rho_{(r)}$ (Table 2). The sign of $(\nabla^2\rho_{(r)})$ at BCP is having significance in discriminating the shared-shell (covalent bond (-ve)) and closed-shell (ionic, van der Waals interaction, and HB (+ve)). From Table 2 it is confirmed that, BCPs other than for molecule **3** are coming under closed-shell (HB) interactions. The BCPs of interest for molecule **3** shows –ve value of $(\nabla^2\rho_{(r)})$ indicating that these interactions as expected are coming under shared-shell. If the calculated strengths of HB in Table 2 are compared with the chemical shifts of NH protons in Table 1, it will become evident that the strength of HB is directly related with chemical shift of NH (H-bonded) proton (downfield shift with increasing strength or *vice versa*). Thus at identical experimental conditions we could compare the relative strengths of HBs by utilizing the NMR chemical shifts.

Relaxed potential energy scan

Relaxed potential energy surface for the internal rotation of the phenyl ring through single bond was performed at B3LYP/6-311G (d, p) level of calculation. The rotation of 360° (-180 – 0 – +180) through single bond was scanned in 20 steps with 18° size of rotational segments. The scanned graph of Energy (kcal/mol) versus Dihedral Angle (θ) is reported in Fig. 9 and the animation of scan is also reported with ESI. From the graph it is clear that the energy of cis conformer is lower than the other, and is maximum for the trans conformation.

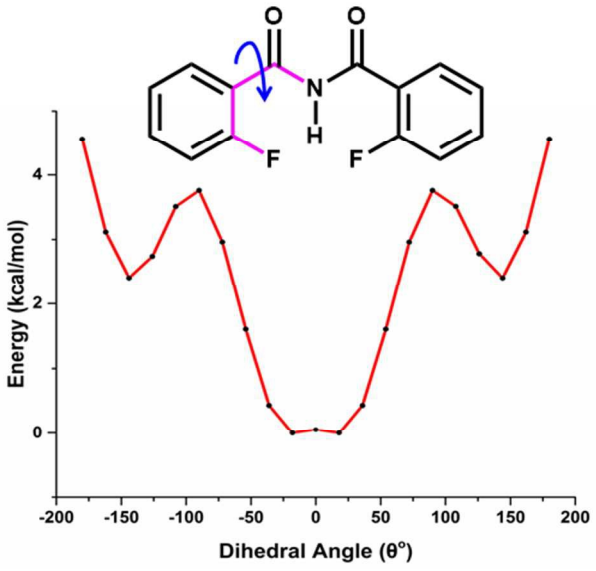

Figure 9: Relaxed potential energy surface for the internal rotation of the phenyl ring through single bond was performed at B3LYP/6-311G (d, p) level of calculation. The dihedral angle and the rotation direction are highlighted in the structure of molecule.

Experimental

The NMR spectra of all the investigated molecules were acquired using Bruker AVANCE 400, 500 and 800 MHz NMR spectrometers. TMS (0.0 ppm) is taken as the internal reference for proton chemical shifts and hexafluorobenzene (-164.9 ppm) is used as internal reference for all ^{19}F spectra. All the NMR spectra for characterization of synthesized molecules were acquired at 298 K. Deuterated solvents, such as, $CDCl_3$, and DMSO-d_6 were purchased from Cambridge Isotopes Limited and used as received. The fresh $CDCl_3$ was used to avoid the possibility of artificial alteration in the interaction, because the strength of non-covalent interactions is found to be dependent on solvent and substrate purity. The molecular mass of the synthesized molecules were confirmed using electrospray ionization high resolution mass spectrometry (ESI-HRMS). The standard programs of Bruker NMR spectrometers library were used to acquire the two dimensional HSQC, HOESY and DOSY spectra.

General procedure for synthesis

Different derivatives of imides were synthesized using the corresponding benzamide and benzoyl chlorides[66]. All the benzamide and benzoyl chlorides of high purity were purchased and used as received. The AR grade solvent n-hexane (C_6H_{14}) chloroform ($CHCl_3$), n-pentane (C_5H_{12}) and HPLC grade methanol (CH_3OH) were used in the purification.

Synthesis of substituted imides

200 mg of corresponding benzamide and the benzoyl chloride of interest were taken in (1:1.2) molar ratio in the silica crucible and mixed using clean spatula. The resulted mixture was exposed in the microwave irradiation at 450 W for 5 min. The reaction was monitored using TLC till completion. For further purification the compound was passed through the column loaded with neutral alumina (Al_2O_3) using the mixture of solvents, n-hexane and chloroform. The gradient of solvent was varied from 5% to 30% chloroform with gradual increment. The obtained product was crystalized using methanol (CH_3OH) and dichloromethane (CH_2Cl_2) in 2:1 ratio.

Conclusions

The combined multinuclear and multidimensional NMR experiments and DFT based theoretical calculations unambiguously establishes the presence of intramolecular HBs in all the investigated fluorine derivatives of imides. Any possibility of self or cross dimerization has been discarded by $CDCl_3$ titration (concentration variation study) and also by ^1H DOSY NMR technique. The ^1H-^{19}F HOESY (heteronuclear through space correlation) experiment indirectly provided the information about the possibility of intramolecular HB. Through space coupling via HB is detected in 1D ^1H and 2D ^1H-^{15}N HSQC, experiments whose magnitudes varied over the range of 6-15 Hz in different fluorine containing molecules. A very sensitive NCI

calculation has been used as a tool for the detection of non-covalent interactions and confirmed the existence of bifurcated intramolecular HBs in the molecules **1-7**. The QTAIM calculations are utilized to derive the energy and strengths of HBs. The calculated energies of HB (E_{HB}) for different investigated molecules are found in the range of -2.07 to -8.92 kcal/mol. The HBs are discriminated from the covalent bonds by using the signs of the Laplacian of electron density. We strongly believe that the present studies lead to a better understanding of the HB in the derivatives of imides and open up the opportunities in designing of the different new drugs, foldamers and supramolecules of pharmacological, chemical and biological importance.

Acknowledgements

SKM would like to thank UGC, New Delhi, for SRF. NS gratefully acknowledges the generous financial supported by Board of Research in Nuclear Sciences, Mumbai (Grant No. 2013/37C/4/BRNS).

Notes and references

Mr. Sandeep Kumar Mishra and Prof. N. Suryaprakash
NMR Research Centre, Solid State and Structural Chemistry Unit,
Indian Institute of Science,
Bangalore-560012 (INDIA)
Tel: 00918022933300; Fax: +918023601550
E-mail: nsp@nrc.iisc.ernet.in

Electronic Supplementary Information (ESI) available: See DOI: 10.1039/b000000x/

References

1. W.-H. Hu, K.-W. Huang, C.-W. Chiou and S.-W. Kuo, *Macromolecules*, 2012, 45, 9020-9028.
2. M. Saccone, V. Dichiarante, A. Forni, A. Goulet-Hanssens, G. Cavallo, J. Vapaavuori, G. Terraneo, C. J. Barrett, G. Resnati, P. Metrangolo and A. Priimagi, *J. Mater. Chem. C*, 2015, 3, 759-768.
3. A. J. P. Teunissen, M. M. L. Nieuwenhuizen, F. Rodríguez-Llansola, A. R. A. Palmans and E. W. Meijer, *Macromolecules*, 2014, 47, 8429-8436.
4. T. Xiao, X. Feng, S. Ye, Y. Guan, S.-L. Li, Q. Wang, Y. Ji, D. Zhu, X. Hu, C. Lin, Y. Pan and L. Wang, *Macromolecules*, 2012, 45, 9585-9594.
5. A. Ajayaghosh, S. J. George and A. P. H. J. Schenning, in *Top. Curr. Chem.* ed. F. Würthner, Springer Berlin Heidelberg, 2005, 258, 135681, 83-118.
6. E. A. Archer, H. Gong and M. J. Krische, *Tetrahedron*, 2001, 57, 1139-1159.
7. L. Brunsveld, B. J. B. Folmer, E. W. Meijer and R. P. Sijbesma, *Chem. Rev.* 2001, 101, 4071-4098.
8. M. M. Conn and J. Rebek, *Chem. Rev.* 1997, 97, 1647-1668.
9. F. Huang and H. W. Gibson, *Prog. Polym. Sci.* 2005, 30, 982-1018.
10. D. S. Lawrence, T. Jiang and M. Levett, *Chem. Rev.* 1995, 95, 2229-2260.
11. O. Lukin and F. Vögtle, *Angew. Chem., Int. Ed.* 2005, 44, 1456-1477.
12. J. S. Nowick, *Acc. Chem. Res.* 1999, 32, 287-296.
13. L. J. Prins, D. N. Reinhoudt and P. Timmerman, *Angew. Chem., Int. Ed.* 2001, 40, 2382-2426.
14. C. Schmuck and W. Wienand, *Angew. Chem., Int. Ed.* 2001, 40, 4363-4369.
15. R. Shenhar and V. M. Rotello, *Acc. Chem. Res.* 2003, 36, 549-561.
16. R. P. Sijbesma and E. W. Meijer, *Chem. Commun.* 2003, DOI: 10.1039/B205873C, 5-16.
17. F. Zeng and S. C. Zimmerman, *Chem. Rev.* 1997, 97, 1681-1712.
18. B. Gong, *Chem. Eur. J.* 2001, 7, 4336-4342.
19. I. Huc, *Eur. J. Org. Chem.* 2004, 2004, 17-29.
20. Z.-T. Li, J.-L. Hou, C. Li and H.-P. Yi, *Chem. Asian J.* 2006, 1, 766-778.
21. J. W. Lockman, N. M. Paul and J. R. Parquette, *Prog. Polym. Sci.* 2005, 30, 423-452.
22. A. R. Sanford, K. Yamato, X. Yang, L. Yuan, Y. Han and B. Gong, *Eur. J. Biochem.* 2004, 271, 1416-1425.
23. I. Muegge, S. L. Heald and D. Brittelli, *J. Med. Chem.* 2001, 44, 1841-1846.
24. B. E. Smart, *J. Fluorine Chem.* 2001, 109, 3-11.
25. D. Chopra and T. N. G. Row, *CrystEngComm*, 2011, 13, 2175-2186.
26. G. R. Desiraju, *J. Am. Chem. Soc.* 2013, 135, 9952-9967.
27. K. Reichenbacher, H. I. Suss and J. Hulliger, *Chem. Soc. Rev.* 2005, 34, 22-30.
28. R. Berger, G. Resnati, P. Metrangolo, E. Weber and J. Hulliger, *Chem. Soc. Rev.* 2011, 40, 3496-3508.
29. R. H. Abeles and T. A. Alston, *J. Biol. Chem.* 1990, 265, 16705-16708.
30. M.-C. Chapeau and P. A. Frey, *J. Org. Chem.* 1994, 59, 6994-6998.
31. T. Kovacs, A. Pabuccuoglu, K. Lesiak and P. F. Torrence, *Bioorg. Chem.* 1993, 21, 192-208.

32. D. O'Hagan and H. S. Rzepa, *Chem. Commun.* 1997, DOI: 10.1039/A604140J, 645-652.
33. L. H. Takahashi, R. Radhakrishnan, R. E. Rosenfield, E. F. Meyer and D. A. Trainor, *J. Am. Chem. Soc.* 1989, 111, 3368-3374.
34. I. Alkorta, J. Elguero, H.-H. Limbach, I. G. Shenderovich and T. Winkler, *Magn. Reson. Chem.* 2009, 47, 585-592.
35. C. Bartolome, P. Espinet and J. M. Martin-Alvarez, *Chem. Commun.* 2007, DOI: 10.1039/B710304B, 4384-4386.
36. S. R. Chaudhari, S. Mogurampelly and N. Suryaprakash, *J. Phys. Chem. B*, 2013, 117, 1123-1129.
37. I. E. Kareev, G. S. Quiñones, I. V. Kuvychko, P. A. Khavrel, I. N. Ioffe, I. V. Goldt, S. F. Lebedkin, K. Seppelt, S. H. Strauss and O. V. Boltalina, *J. Am. Chem. Soc.* 2005, 127, 11497-11504.
38. G. K. S. Prakash, F. Wang, M. Rahm, J. Shen, C. Ni, R. Haiges and G. A. Olah, *Angew. Chem.*, *Int. Ed.* 2011, 50, 11761-11764.
39. R. Banerjee, G. R. Desiraju, R. Mondal and J. A. K. Howard, *Chem. Eur. J.* 2004, 10, 3373-3383.
40. C. Li, S.-F. Ren, J.-L. Hou, H.-P. Yi, S.-Z. Zhu, X.-K. Jiang and Z.-T. Li, *Angew. Chem.*, *Int. Ed.* 2005, 44, 5725-5729.
41. Y. Mido and T. Okuno, *J. Mol. Struct.* 1982, 82, 29-34.
42. H. Takemura, N. Kon, M. Yasutake, S. Nakashima, T. Shinmyozu and T. Inazu, *Chem. Eur. J.* 2000, 6, 2334-2337.
43. X. Zhao, X.-Z. Wang, X.-K. Jiang, Y.-Q. Chen, Z.-T. Li and G.-J. Chen, *J. Am. Chem. Soc.* 2003, 125, 15128-15139.
44. K. Divya, S. Hebbar and N. Suryaprakash, *Chem. Phys. Lett.* 2012, 525–526, 129-133.
45. G. N. Manjunatha Reddy, M. V. Vasantha Kumar, T. N. Guru Row and N. Suryaprakash, *Phys. Chem. Chem. Phys.* 2010, 12, 13232-13237.
46. D. Chopra, *Cryst. Growth Des.* 2011, 12, 541-546.
47. J. D. Dunitz, *ChemBioChem*, 2004, 5, 614-621.
48. J. D. Dunitz and R. Taylor, *Chem. Eur. J.* 1997, 3, 89-98.
49. J. A. K. Howard, V. J. Hoy, D. O'Hagan and G. T. Smith, *Tetrahedron*, 1996, 52, 12613-12622.
50. I. D. Rae, J. A. Weigold, R. H. Contreras and R. R. Biekofsky, *Magn. Reson. Chem.* 1993, 31, 836-840.
51. H. Benedict, I. G. Shenderovich, O. L. Malkina, V. G. Malkin, G. S. Denisov, N. S. Golubev and H.-H. Limbach, *J. Am. Chem. Soc.* 2000, 122, 1979-1988.
52. N. S. Golubev, I. G. Shenderovich, S. N. Smirnov, G. S. Denisov and H.-H. Limbach, *Chem. Eur. J.* 1999, 5, 492-497.
53. I. G. Shenderovich, S. N. Smirnov, G. S. Denisov, V. A. Gindin, N. S. Golubev, A. Dunger, R. Reibke, S. Kirpekar, O. L. Malkina and H.-H. Limbach, *Phys. Chem.* 1998, 102, 422-428.
54. I. G. Shenderovich, P. M. Tolstoy, N. S. Golubev, S. N. Smirnov, G. S. Denisov and H.-H. Limbach, *J. Am. Chem. Soc.* 2003, 125, 11710-11720.
55. S. K. Mishra and N. Suryaprakash, *Phys.Chem.Chem.Phys*. 2015, 17, 15226—15235.
56. A. Lakshmipriya, S. R. Chaudhari, A. Shahi, E. Arunan and N. Suryaprakash, *Phys.Chem.Chem.Phys*. 2015, 17, 7528—7536.
57. IUPAC. *Compendium of Chemical Terminology,* 2nd ed. *(the "Gold Book").* Compiled by A. D. McNaught and A. Wilkinson. *Blackwell Scientific Publications, Oxford* 1997. XML on-line corrected version: http://goldbook.iupac.org, 2006, created by M. Nic, J. Jirat, B. Kosata; updates compiled by A. Jenkins. ISBN 0-9678550-9-8. doi:10.1351/goldbook.
58. W. W. Walter and H. A. Michael *"Polyimides" in Ullmann's Encyclopedia of Industrial Chemistry,* 2002, Wiley-VCH, Weinheim. doi:10.1002/14356007.a21_253.
59. J. Prinos, Ch. Tselios, D. Bikiaris and C. Panayiotou, *Polymer*, 1997, 38, 5921-5930.
60. L. Luo, Y. Zheng, J. Huang, K. Li, H. Wang, Y. Feng, X. Wang and X. Liu, *J. Appl. Polym. Sci.* 2015, 132, n/a, DOI: 10.1002/APP.42001.
61. Y. Kanaoka, *Acc. Chem. Res.*, 1978, **11**, 407-413.
62. J. Stec, Q. Huang, M. Pieroni, M. Kaiser, A. Fomovska, E. Mui, W. H. Witola, S. Bettis, R. McLeod, R. Brun and A. P. Kozikowski, *J. Med. Chem.*, 2012, **55**, 3088-3100.
63. H. Wang, S. P. Kelley, J. W. Brantley, G. Chatel, J. Shamshina, J. F. B. Pereira, V. Debbeti, A. S. Myerson and R. D. Rogers, *ChemPhysChem*, 2015, 16, 993–1002.
64. D. Sprecher, M. Maxwell, J. Goodman, B. White, C.-M. Tang, V. Boullay and A.-C. de Gouville, *Eur. J. Pharmacol.*, 2015, 756, 1–7
65. R. Mhidia, E. Boll, F. Fécourt, M. Ermolenko, N. Ollivier, K. Sasaki, D. Crich, B. Delpech and O. Melnyk, *Bioorg. Med. Chem.*, 2013, **21**, 3479-3485.
66. Y. Li, Y. Wang and J. Wang, *Russ. J. Organ. Chem.*, 2008, 44, 358-361.
67. S. Ahmad, K. M. Ali, J. Charalambous and M. J. Frazer, *Inorg. Chim. Acta.*, 1978, **31**, 69-76.
68. W. Kohn and L. J. Sham, *Phys. Rev*. 1965, 140, A1133-A1138.
69. R.G. Parr and W. Yang, *Density-Functional Theory of Atoms and Molecules, Oxford University Press, New York,* 1989.
70. J. Contreras-García, W. Yang and E. R. Johnson, *J. Phys. Chem. A*, 2011, 115, 12983-12990.
71. R. F. W. Bader, *Atoms in Molecules: A Quantum Theory*, Oxford University Press, Oxford, **1990.**
72. A. E. Reed, L. A. Curtiss and F. Weinhold, *Chem. Rev.* 1988, 88, 899-926.
73. M. Nakahara and C. Wakai, *Chem. Lett.* 1992, 21, 809-812.
74. S. H. Gellman, B. R. Adams and G. P. Dado, *J. Am. Chem. Soc.* 1990, 112, 460-461.
75. S. H. Gellman, G. P. Dado, G. B. Liang and B. R. Adams, *J. Am. Chem. Soc.* 1991, 113, 1164-1173.
76. F. J. Martinez-Martinez, A. Ariza-Castolo, H. Tlahuext, M. Tlahuextl and R. Contreras, *J. Chem. Soc., Perkin Trans. 2*, 1993, DOI: 10.1039/P29930001481, 1481-1485.
77. J. R. Cheeseman, G. W. Trucks, T. A. Keith, and M. J. Frisch, *J. Chem. Phys.* 1996, 104, 5497-5509.
78. K. F. Morris and C. S. Johnson, *J. Am. Chem. Soc.* 1992, 114, 3139-3141.
79. K. F. Morris and C. S. Johnson, *J. Am. Chem. Soc.* 1993, 115, 4291-4299.
80. T. Axenrod, P. S. Pregosin, M. J. Wieder, E. D. Becker, R. B. Bradley and G. W. A. Milne, *J. Am. Chem. Soc.* 1971, 93, 6536-6541.
81. A. J. Dingley, J. E. Masse, R. D. Peterson, M. Barfield, J. Feigon and S. Grzesiek, *J. Am. Chem. Soc.* 1999, 121, 6019-6027.

82. A. Dunger, H.-H. Limbach and K. Weisz, *J. Am. Chem. Soc.* 2000, 122, 10109-10114.
83. S. Grzesiek, F. Cordier, V. Jaravine and M. Barfield, *Prog. Nucl. Magn. Reson. Spectrosc.* 2004, 45, 275-300.
84. A. V. Afonin, I. A. Ushakov, L. N. Sobenina, Z. V. Stepanova, O. g. V. Petrova and B. A. Trofimov, *Magn. Reson. Chem.* 2006, 44, 59-65.
85. M. M. King, H. J. C. Yeh and G. O. Dudek, *Org. Magn. Reson.* 1976, 8, 208-212.
86. P. L. Rinaldi, *J. Am. Chem. Soc.* 1983, 105, 5167-5168.
87. C. Yu and G. C. Levy, *J. Am. Chem. Soc.* 1983, 105, 6994-6996.
88. C. Yu and G. C. Levy, *J. Am. Chem. Soc.* 1984, 106, 6533-6537.
89. M. J. Frisch, G. W. Trucks, H. B. Schlegel, G. E. Scuseria, M. A. Robb, J. R. Cheeseman, G. Scalmani, V. Barone, B. Mennucci, G. A. Petersson, H. Nakatsuji, M. Caricato, X. Li, H. P. Hratchian, A. F. Izmaylov, J. Bloino, G. Zheng, J. L. Sonnenberg, M. Hada, M. Ehara, K. Toyota, R. Fukuda, J. Hasegawa, M. Ishida, T. Nakajima, Y. Honda, O. Kitao, H. Nakai, T. Vreven, J. A. Montgomery Jr., J. E. Peralta, F. Ogliaro, M. J. Bearpark, J. Heyd, E. N. Brothers, K. N. Kudin, V. N. Staroverov, R. Kobayashi, J. Normand, K. Raghavachari, A. P. Rendell, J. C. Burant, S. S. Iyengar, J. Tomasi, M. Cossi, N. Rega, N. J. Millam, M. Klene, J. E. Knox, J. B. Cross, V. Bakken, C. Adamo, J. Jaramillo, R. Gomperts, R. E. Stratmann, O. Yazyev, A. J. Austin, R. Cammi, C. Pomelli, J. W. Ochterski, R. L. Martin, K. Morokuma, V. G. Zakrzewski, G. A. Voth, P. Salvador, J. J. Dannenberg, S. Dapprich, A. D. Daniels, Ö. Farkas, J. B. Foresman, J. V. Ortiz, J. Cioslowski and D. J. Fox, Gaussian, Inc., Wallingford, CT, USA, 2009.
90. E. R. Johnson, S. Keinan, P. Mori-Sánchez, J. Contreras-García, A. J. Cohen and W. Yang, *J. Am. Chem. Soc.* 2010, 132, 6498-6506.
91. T. Lu and F. Chen, *J. Comput. Chem.* 2012, 33, 580-592.
92. W. Humphrey, A. Dalke and K. Schulten, *J. Molec. Graphics* 1996, 14, 33-38.
93. R. F. W. Bader, S. G. Anderson and A. J. Duke, *J. Am. Chem. Soc.* 1979, 101, 1389-1395.
94. R. F. W. Bader and H. Essén, *J. Chem. Phys.* 1984, 80, 1943-1960.
95. R. F. W Bader, T. T. Nguyen-Dang, and Y. Tal, *Rep. Prog. Phys.* 1981, 44, 893-948;
96. G. R. Runtz, R. F. W. Bader and R. R. Messer, *Can. J. Chem.* 1977, 55, 3040-3045.
97. E. Espinosa, E. Molins and C. Lecomte, *Chem. Phys. Lett.* 1998, 285, 170-173.